*Molecular Vision* 2020; 26:299-310 <http://www.molvis.org/molvis/v26/299>
Received 30 April 2019 | Accepted 14 April 2020 | Published 16 April 2020



# A unique *PRDM13*-associated variant in a Georgian Jewish family with probable North Carolina macular dystrophy and the possible contribution of a unique *CFH* variant

**Prasanthi Namburi,[1] Samer Khateb,[1] Segev Meyer,[1] Tom Bentovim,[1] Rinki Ratnapriya,[2] Alisa Khramushin,[3] Anand Swaroop,[2] Ora Schueler-Furman,[3] Eyal Banin,[1] Dror Sharon[1]**

**(The first two authors contributed equally to this study.)**

*[1]Department of Ophthalmology, Hadassah Medical Center, Faculty of Medicine, The Hebrew University Jerusalem, Jerusalem, Israel; [2]Neurobiology-Neurodegeneration & Repair Laboratory, National Eye Institute, National Institutes of Health, Bethesda, MD; [3]Department of Microbiology and Molecular Genetics, IMRIC, Faculty of Medicine, Hebrew University of Jerusalem, Israel*

**Purpose:** North Carolina macular dystrophy (NCMD) is an autosomal dominant maculopathy that is considered a non-progressive developmental disorder with variable expressivity. Our study aimed to clinically and genetically characterize macular dystrophy in a family (MOL1154) consisting of six affected subjects with a highly variable maculopathy phenotype in which no correlation between age and severity exists.

**Methods:** Clinical characterization included visual acuity testing and electroretinography. Genetic analysis included Sanger sequencing and whole exome sequencing (WES).

**Results:** WES analysis performed on DNA samples from two individuals revealed a heterozygous deletion of six nucleotides [c.2247_2252del; p.(Leu750_Lys751del)] in the *CFH* gene. Co-segregation analysis revealed that five of the six NCMD affected subjects carried this deletion, while one individual who had a relatively mild phenotype compatible with dry age-related macular degeneration (AMD) did not carry it. We subsequently analyzed the upstream region of *PRDM13* that has previously been reported to be associated with NCMD and identified a unique heterozygous transversion (chr6:100040974A>C) located within the previously described suspected control region in all six affected individuals. This transversion is likely to cause NCMD.

**Conclusions:** NCMD has a wide spectrum of clinical phenotypes that can overlap with AMD, making it challenging to correctly diagnose affected individuals and family members. The DNA sequence variant we found in the *CFH* gene of some of the affected family members may suggest some role as a modifier gene. However, this variant still does not explain the huge phenotypic variability of NCMD and needs to be studied in other and larger populations.

Inherited macular diseases include a wide range of complex entities characterized by bilateral visual loss with significant macular abnormalities and belong to a larger group of inherited retinal diseases (IRDs). In many cases, the disease pathogenesis remains unclear. Considerable clinical and genetic heterogeneity is evident in IRDs, and various inheritance patterns, including autosomal dominant (AD), autosomal recessive (AR), and X-linked (XL) patterns, have been reported.

North Carolina macular dystrophy (NCMD; OMIM 136550) is a unique congenital macular dystrophy with an AD inheritance pattern [1]. Originally, NCMD was reported in a single family living in the mountains of North Carolina, and therefore the disease was named after the founder effect of this family [2,3]. NCMD is a non-progressive disorder characterized by a variable macular phenotype with a few small (less than 50 µm) yellow drusen-like lesions in the macular center in grade I, larger confluent lesions in grade II, and macular colobomatous lesions in grade III [4].

The original NCMD family disease was mapped by Small et al. [1] using genetic linkage analysis of chromosome 6q16 and was named MCDR1 (MC = macula, D = dystrophy, R = retina 1 = first one mapped) by the Human Genome Organization. Subsequently, multiple new NCMD families worldwide were found to be mapped to chromosome 6q16 [5-7]. Subsequently, the NCMD phenotype in a Danish family was mapped to chromosome 5 (MCDR3, MIM:608850) [8-10]. Using whole-genome sequencing, Small et al. found four rare mutations in a non-coding region of the MCDR1 locus [11]. Three were single base substitutions in a DNASE1 hypersensitivity site between CCNC and PRDM13. A large family from Belize was found to have a large duplication involving PRDM13 and the DNASE1 site. The Danish MCDR3 family was found to have a large duplication involving IRX1 and

Correspondence to: Dror Sharon, Hadassah Medical Center, Ein-Kerem, POB 12000, Jerusalem, Israel, 91120; Phone: 972-26777112; FAX: 972-26448917; email: dror.sharon1@mail.huji.ac.il

another DNASE1 site. This was the first study that provided strong evidence of the role of PRDM13 dysregulation in NCMD pathogenesis [11]. These observations were further supported by the identification of a different tandem duplication of *PRDM13* as the cause of NCMD [12]. By studying additional MCDR3-linked families, two distinct heterozygous tandem duplications at the MCDR3 locus, including the *IRX1* and *ADAMTS16* genes, were reported [9]. It should be noted that several macular dystrophies have common clinical and histopathological features similar to age-related macular degeneration (AMD) [13]. The clinical findings of NCMD grade 1 can be indistinguishable from those of AMD, particularly if the subject is elderly.

Here, we present the clinical and genetic characterization of a family with AD maculopathy with marked clinical variability. Two variants, one in the *PRMD13* suspected control region and the other in *CFH*, were variably found in this small family with this disease.

## METHODS

*Clinical characterization:* The study was approved by the Hadassah medical center Institutional Review Board (IRB) and was carried out according to the Declaration of Helsinki. Subjects provided their written consent after receiving an explanation of the purpose of the study. Eight members of a family with macular dystrophy (MOL1154) underwent a comprehensive ocular examination, including best-corrected visual acuity (BCVA) testing, electroretinography (ERG), electrooculography (EOG), color vision testing using the Farnsworth D-15 panel and Ishihara tests, perimetry using the SITA-fast strategy (white target III), spectral-domain optical coherence tomography (SD-OCT), short-wave fundus autofluorescence (SWAF) imaging, and fluorescein angiography (FA) [14].

*Genetic analysis:* Blood samples were collected from each participant, and genomic DNA was isolated using a Maxwell® 16 Blood DNA Purification Kit (Promega, Madison, WI). Whole exome sequencing (WES) was performed on the genomic DNA samples of the index case (MOL1154 IV:2) and her father (MOL1154 III:2) using exomic libraries prepared using a Nextera Rapid Capture Expanded Exome Kit on a HiSeq2500 platform (Illumina, San Diego, CA). The raw sequence data files were evaluated and aligned to the human reference sequence (hg19, GRCH37) using Burrows-Wheeler Aligner (BWA), variants were identified using the GATK pipeline, and the annotation of variants was done using ANNOVAR software. The following filtering steps were implemented: (1) Only heterozygous variants that were present in the index case and absent in the unaffected father were included. (2) Missense, nonsense, frameshift indels, inframe indels, and canonical splice-site variants were included; synonymous variants were excluded. (3) Variants with minor allele frequency > 0.005 were excluded (4). In addition, online prediction tools (Polymorphism Phenotyping v2 (PolyPhen-2); Sorting intolerant from tolerant (SIFT), and MutationTaster) were used to prioritize missense variants.

Sanger sequencing of the entire exonic (and immediate intronic) region of *CFH* and the previously described suspected control region of *PRDM13* was performed on the DNA sample of the index case. PCR primers to amplify and sequence the *CFH* exons were designed using Primer3 Plus software. Primers for the suspected control region of *PRDM13* were reported previously [11] (Appendix 1). The amplified PCR products were analyzed by Sanger sequencing to confirm the presence of identified variants. In addition, PCR analysis of the reported copy number variation of the MCDR1 locus was performed as previously described [11].

*Multiple sequence alignment and structural modeling:*

**Generation of multiple sequence alignments—**Homologous sequences were obtained from HomoloGene. Sequence conservation was determined based on the multiple sequence alignment.

*Generation of structural models of the CFH deletion mutant and estimation of the effect on structural organization and stability:* The Rosetta Macromolecular Modeling suite [15] was used to generate models of the deletion mutant and for the structure-based estimation of the effects on protein stability. Modeling the deletion involved three steps (see Appendix 1 for more details). First, clashes in the structures were removed by a minimization constrained to the starting structure to prevent large moves. Second, kinematic loop closure [16] was used to remodel the linker region of both the wild type (wt) and the deletion mutant (in which the linker loop was shortened by the two CFH residues L750 and K751). For each of the 20 minimized structures (one for each nuclear magnetic resonance [NMR] model), 20 loop closure attempts were made, and the top-scoring model was chosen. Finally, the models were minimized to adjust the relative orientation of the two domains. The energies of the lowest-scoring structures for the wt and the deletion mutant were compared to estimate the loss in stability. The effect of point mutations was estimated using the Rosetta ddG monomer application [17]. Visual inspection and the generation of figures of structures were performed using Pymol.

## RESULTS

MOL1154 is a Georgian Jewish family consisting of six affected subjects from four generations (Figure 1) who underwent comprehensive ocular examinations. Five of the subjects were diagnosed with NCMD and one with AMD. The index case (MOL1154 IV:2) was a female who was 7 years old (YO) when referred to our retina clinic due to suboptimal visual acuity identified in a school screening test. On examination, BCVA was measured as 0.70 Snellen in both eyes (BE). The anterior segments were unremarkable, and there were yellowish macular lesions surrounded by refractile drusen-like dots and RPE atrophy (Table 1). A perimetry test showed generalized visual field depression and a central scotoma involving the fixation point in the left eye (LE) but not in the right eye (RE). Ancillary Ishihara and Farnsworth D-15 tests showed normal color vision; a full field electroretinography (ffERG) test showed normal rod and cone responses; and an electrooculography (EOG) test showed normal RPE function. Two years later, the BCVA was 0.80 Snellen in BE with no change in ocular findings. Horizontal cross-sectional spectral domain optical coherence tomography (SD-OCT) images showed preservation of the ellipsoid zone and thickening of the inter-digitation layer in addition to RPE atrophy corresponding to the yellowish macular lesion borders. Microperimetry showed relatively unstable fixation compatible with the index case's maculopathy. Her 34 YO mother (MOL1154 III:1) started to complain of blurred vision at the age of 25. BCVA was 1.0 and 1.25 Snellen in the RE and LE, respectively. An ocular examination showed unremarkable anterior segments. SD-OCT showed overall preservation of the retinal layers except for subtle inter-digitation layer irregularity compatible with the drusen-like deposits (Figure 2), and small drusen-like lesions engirdling the fovea were evident in BE (Figure 3), resulting in a hyper autofluorescence dot-like pattern surrounding the fovea fixation test results in this case were within the low range of stable fixation. The 28 YO aunt (MOL1154 III:3), who had an unremarkable medical history, presented with asymmetric findings in BE, including BCVA of 0.10 and 1.0 in the RE and the LE, respectively. The anterior segments were within normal limits, but fundoscopy showed a diffuse atrophic retina with pigmentary dots and patches involving the macula (RE) and a yolk-like lesion surrounded by atrophic retina temporal to the fovea (LE). OCT scans were not available for this subject. The 64 YO grandmother (MOL1154 II:2) had a previous systemic history of hypertension, an ocular history of anisometropia, and RE amblyopia. BCVA was 0.30 Snellen in the RE and 0.80 Snellen in the LE. Fundoscopy revealed confluent yellowish spots involving the macula and the periphery combined with RPE atrophy, which appear as hyper-fluorescent lesions in short-wave autofluorescence photos, These were reflected by SD-OCT as a disruption of the inter-digitation layer combined with subfoveal pseudodrusens mainly in the RE (Figure 2 and Figure 3). The oldest subject was the 87 YO great grandmother (MOL1154 I:2) who had a previous medical history of atrial fibrillation treated with warfarin anticoagulation therapy. On examination, BCVA was 0.20 and 0.60 (RE and LE, respectively); BE were observed to have pseudophakia and macular and peripheral drusens compatible with dry AMD. Of note, all affected subjects presented variable phenotype expressivity with no correlation between age and disease severity other than phenotype anticipation. In the younger patients (MOL1154 IV:2 and III:3), severe atrophic scarring was observed, whereas in older patients (MOL1154 III:1, II:4, and II:2), macular atrophic changes were mild and late onset. In addition, significant asymmetry was observed between the two eyes in terms of both BCVA and fundoscopic findings in three of the five affected subjects (Table 1). Macular lesions were congruent with NCMD.

To identify the disease-causing mutation, we performed WES on the DNA samples of the index case and her unaffected father. The analysis revealed 19,003 variants in the index case (MOL1154 IV:2) and 22,062 variants in her father (MOL1154 III:2), with an average coverage of 48 reads per nucleotide. Among all variants, 3211 were prioritized based on an autosomal dominant inheritance pattern (heterozygous variants that are present in the index case and absent in her unaffected father). Following filtering steps as detailed in the Methods section, we were able to reduce the list of candidate variants to 25 (Appendix 1) and then to 8, 5 of which were predicted to be deleterious by online prediction tools (PolyPhen 2, SIFT, and MutationTaster; Appendix 1). Finally, the possible sequence variants in genes that were previously reported to be associated with IRDs were studied, and a heterozygous variant, c.2247_2252del; p.(Leu750_Lys751del) that is absent from the gnomAD database was identified in exon 15 of the complement factor H *(CFH)* gene (Figure 4B). This variant was present in five of the six affected subjects (MOL1154 I:2, who had a relatively mild phenotype that is compatible with AMD, did not carry it). Multiple sequence alignment revealed that the two deleted amino acids are highly conserved among species (Figure 5). Structural inspection of the NMR solved structure of the tandem CPP12–13 repeat (pdb ID 2KMS [18]) revealed that the deletion is located in the connecting linker (residues 746–751 AIDKLK); L750 is positioned at the center of a small hydrophobic core formed by residues in CPP12 (T724, I726) and the linker (V745, I747, K749, L750), which stabilizes the relative orientation between CPP12 and CPP13 (Figure 6A). To estimate the effect of the L750-K751 deletion on protein structure and stability, we

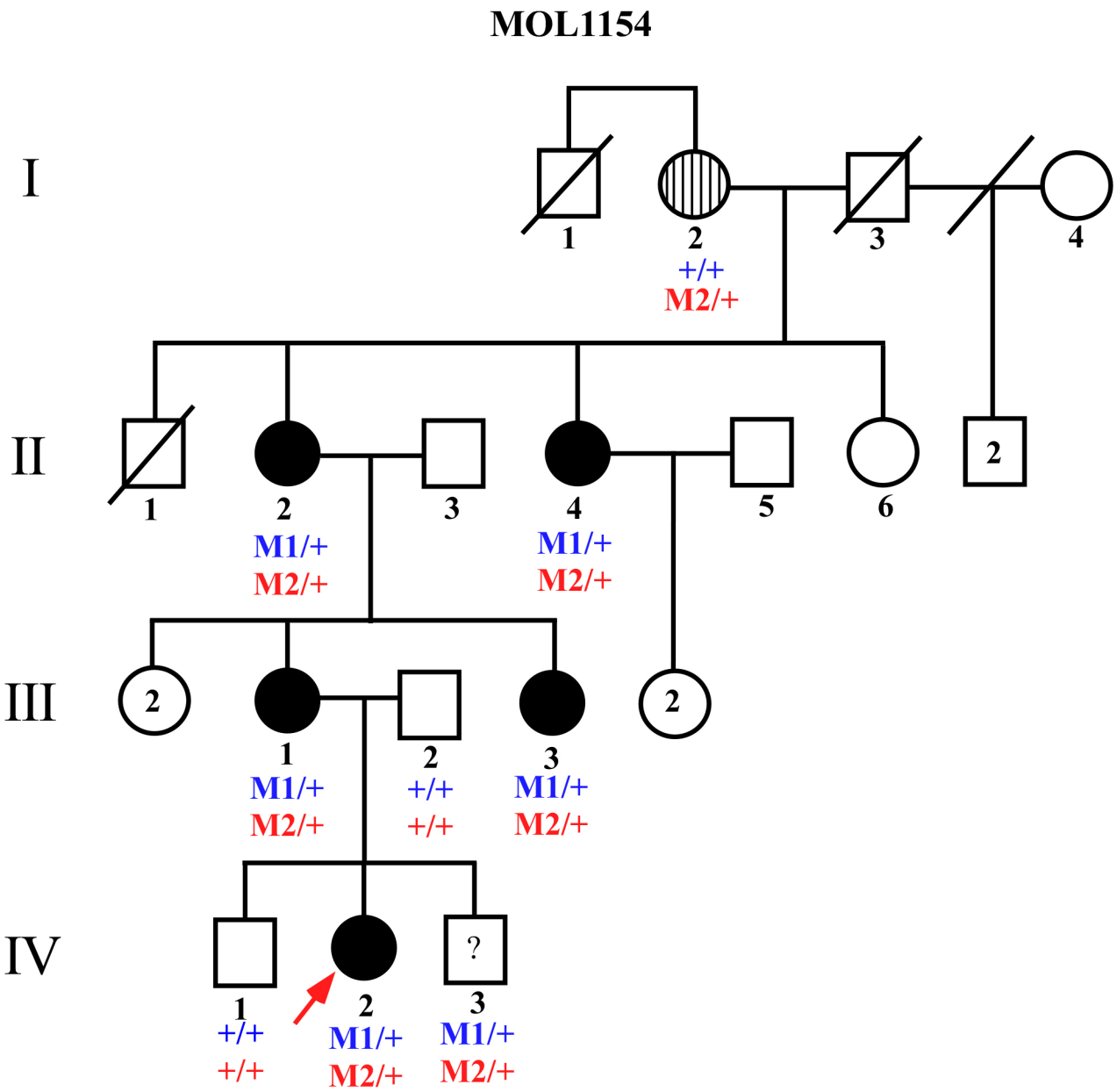


Figure 1. Pedigree of the MOL1154 family. Filled symbols designate affected individuals. The hatched round symbol represents an affected case with a milder phenotype. A square with a question mark symbol represents an individual who participated in genetic analysis, but clinical examination was not performed due to their young age. The red arrow represents the index case. The individual number is depicted below each symbol. The identified variants are depicted below the individual number: M1: *CFH* - c.2247_2252del; p.(Leu750_Lys751del), M2: chr6:100040974A>C, +: wild-type allele.

modeled the structure of the mutant protein and compared it to the corresponding structure of the wt protein using a procedure of three consecutive steps (see Methods and Appendix 1 for more details). After the removal of clashes, the linker (residues $_{746}$AIDKLKK$_{752}$ in the wt and residues $_{746}$AIDKK$_{750}$ in the deletion mutant) was rebuilt followed by minimization that allowed the relative orientation of the two domains to adjust. The structural models of the wt and mutant proteins reveal how the hydrophobic patch centered around L750 is destabilized upon its removal. In the mutant, the shortened linker positions D748 at the same site, thereby changing the hydrophobic side chain character to a negative charge, which

Table 1. Summary of clinical data of patients included in this analysis.

| Patient ID | Age | Sex | BCVA | Anterior segment | Lens | Fundus |
|---|---|---|---|---|---|---|
| MOL1154 IV:2 | 10 | F | 0.70 | Normal | Clear | Macular lesion with peripheral refractile drusen-like dots |
| MOL1154 III:3 | 28 | F | 0.55 | Normal | Clear | Macular lesions |
| MOL1154 III:1 | 34 | F | 1.10 | Normal | Clear | Macular drusen-like lesions |
| MOL1154 II:4 | 57 | F | NA | NA | NA | Confluent drusen-like cluster within the fovea |
| MOL1154 II:2 | 62 | F | 0.55 | Normal | Clear | Macular and peripheral yellow spots |
| MOL1154 I:2 | 87 | F | 0.40 | Normal | Clear | Macular and peripheral drusen |

NA-data not available.

significantly destabilizes the structure ($\Delta\Delta G_{WT,mut}$ = -15.73 Rosetta energy units [REU]; Figures 6A,B).

To estimate the contribution of the L750 side chain to stability, we performed computational point mutations of L750 to alanine (reflecting the removal of the L750 side chain) and aspartate (reflecting the local environment predicted for the mutant). The calculated changes in binding energy show similar results, indicating that indeed the interaction of the L750 side chain with the local hydrophobic patch is the main contribution of this residue to stability compared to the corresponding D748 side chain ($\Delta\Delta G_{WT,L750A}$ = -7.31REU; $\Delta\Delta G_{WT,L750D}$ = -17.26REU). Destabilization of this hydrophobic patch could well lead to changes in the relative orientation of the two domains. While the solved NMR structural models show some variation in orientation, this variation increases in the deletion mutant (Figures 6C,D).

A report by Small et al. regarding the involvement of *PRDM13* in macular development [11] concentrated our focus on the role of *PRDM13* in the MOL1154 family. Therefore, we screened genomic areas reported to include mutations in the vicinity of *PRDM13* and identified a novel heterozygous transversion (hg19; chr6: 100040974A > C) located within the previously described suspected control region. This variant segregated in the six affected individuals and was found in one questionably unaffected child (IV:3) and could not be found in 1000 Genomes and gnomAD. In addition, we screened 21 index cases that suffer from maculopathy (age range 15–65, 52% males, 75% sporadic and 25% AD, most pre-screened for IRD founder mutations in the appropriate population) and did not identify any possible *PRDM13*-related pathogenic variants.

## DISCUSSION

The current study investigated a four-generation macular dystrophy family that has phenotypic variability consistent with NCMD. The oldest affected subject, I:2, has clinical findings suggestive of AMD and a phenocopy.

Our initial WES analysis revealed a heterozygous deletion of six nucleotides (c.2247_2252del) in *CFH*. This variant, which would be expected to contribute to the AMD phenotype, was not present in the oldest affected subject, I:2. Another hypothesis is that the *CHF* variant may be acting as a modifier gene on *PRDM13*.

CFH is a 155 kDa protein that is an abundant plasma glycoprotein [19-21] composed of 20 repetitive units. Each repetitive unit contains short consensus repeats (SCRs) or complement control protein modules (CCPs) that span approximately 60 residues (51–62 residues) [21] (Figure 4A). *CFH* consists of 23 exons, where each repetitive unit is usually encoded by a single exon. Exon 1 encodes 18 amino acids at the N-terminal end for signal peptide formation; exons 3 and 4 together encode a single CCP; exon 10 does not participate in the synthesis of the *CFH* transcript but compensates in alternative transcript formation that encodes for factor H-like protein 1 (FHL-1) [22]. To understand the effect of the identified p.(Leu750_Lys751del) variant on protein function, we inspected the NMR solution structure of CCPs 12 and 13 that span the deletion in the linker between the two CCP domains (2KMS [18]; Figure 6A). It has previously been reported that this central part of the repeat region in CFH (CCPs 12–14) forms a kink that allows the two ends (CCPs 1–6 and CCPs 19–20) to come together [23]. Indeed, the multiple sequence alignment indicates that the deleted amino acids (Leu750 and Lys751) are part of a highly conserved region among different species (Figure 5), which also includes residues Thr724, Ile726, Val745, Ala746, Ile747, Leu750, His773, and Asn794 that have been previously reported as key interface residues

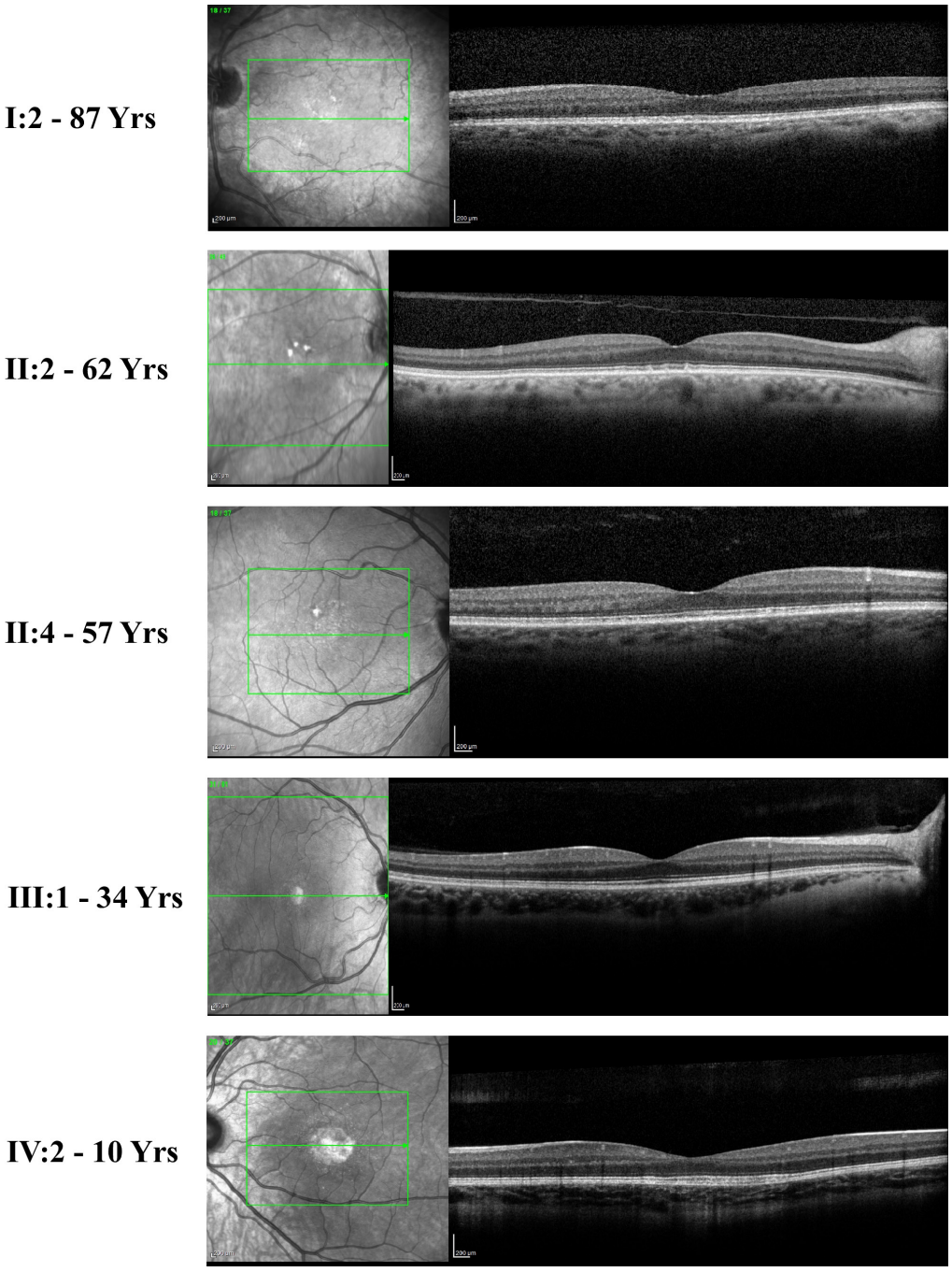


Figure 2. OCT images of affected family members. Representative OCT scans of five affected individuals are shown. Individual numbers and the age in years are shown on the left. MOL1154 I:2 - preserved inner retinal layer combined with granular interdigitation layer. MOL1154 II:2 and II:4 - pseudodrusens with intact outer and inner retinal layers. MOL1154 III:1- OCT cross-sections show normal retinal structure. Note that drusen-like deposits were seen clinically but do not appear in the OCT sections. MOL1154 IV:2 - subfoveal RPE atrophy combined with thickening of the interdigitation layer, while the ellipsoid layer seems to be intact.

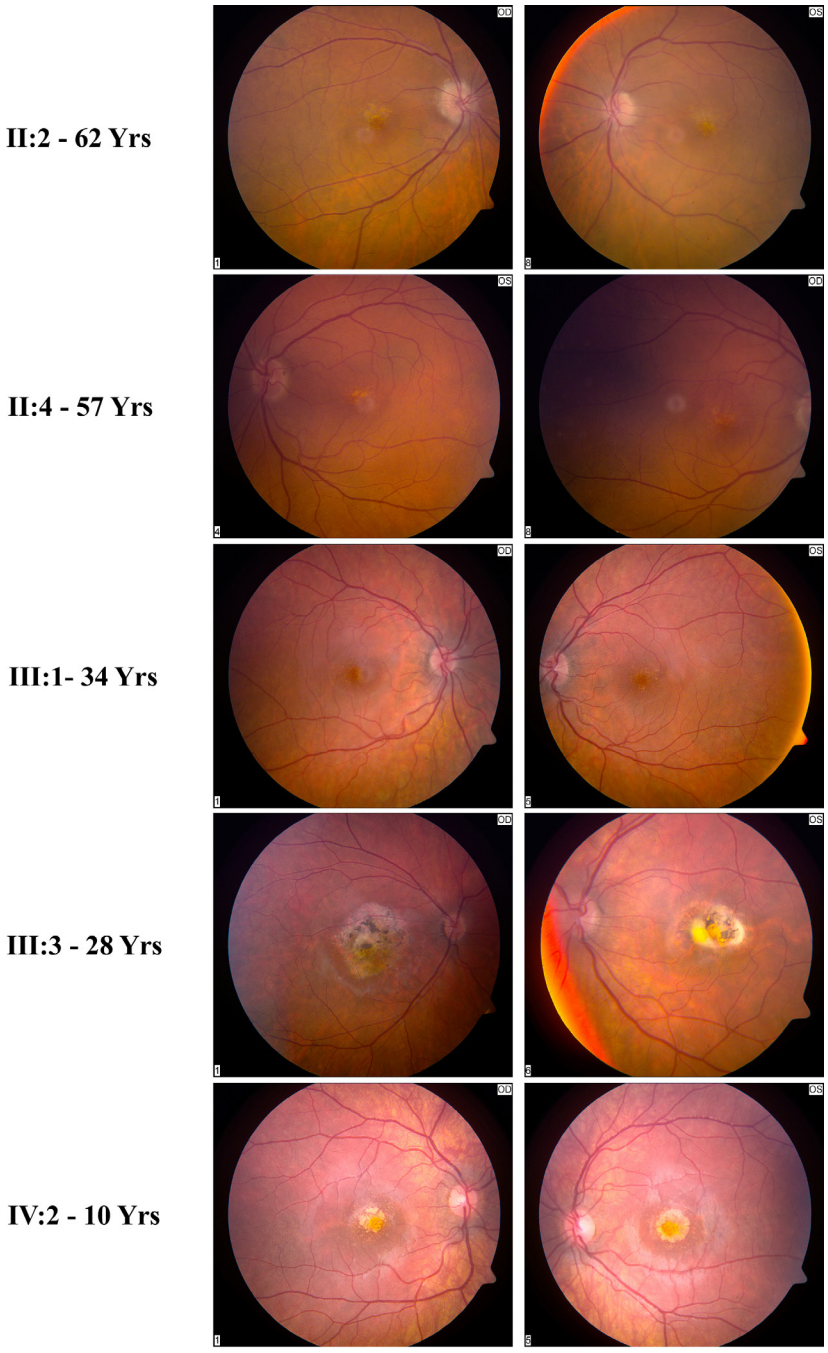


Figure 3. Retinal imaging by fundoscopy of affected members. Representative color fundus photos of five affected individuals are shown. Individual numbers and the age in years are shown on the left. MOL1154 III:1, II:4, and II:2 - confluent foveal drusen-like clusters, while no significant findings are evident in the periphery. MOL1154 III:3 - advanced macular atrophy in both eyes with pigmentary dots and patches in RE and a yolk-like lesion surrounded by atrophic retina temporal to the fovea in LE. MOL1154 IV:2 - refractile drusen-like dots surrounding macular atrophy containing yellowish deposits. OD (oculus dextrus) - right eye; OS (oculus sinister) - left eye.

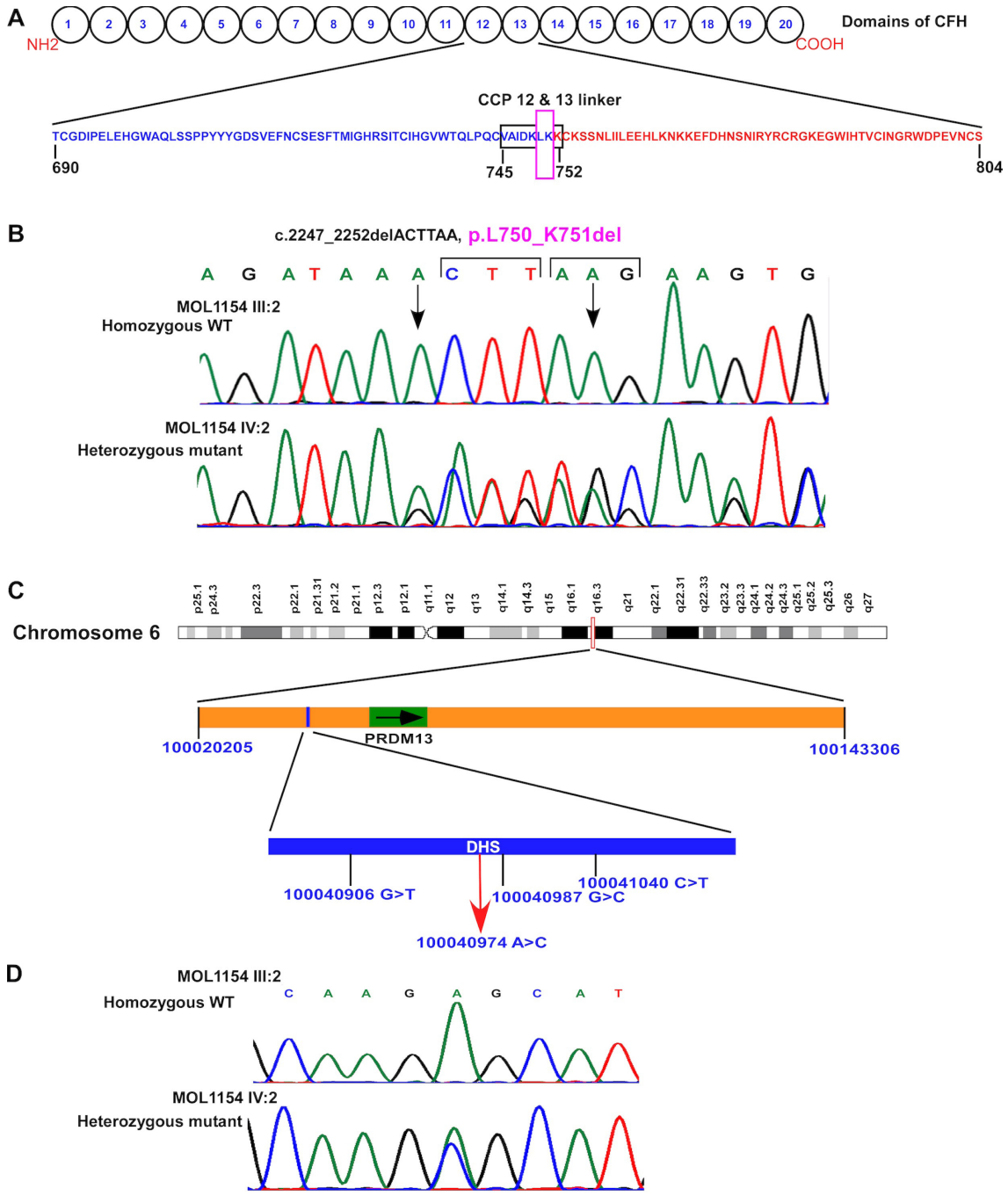


Figure 4. Identified genetic variants. **A**: Domains of the CFH protein that is composed of 20 repetitive units of 60 amino acids called short consensus repeats (SCRs) or complement control protein modules (CCPs). The amino acid sequence of CCPs 12 (blue color) and 13 (red color) are depicted (690–804). The eight residues that are in the black box are located in the CCP 12 and 13 linker region. The pink colored box shows amino acid residues that were found to be deleted in our study. **B**: Chromatograms of a homozygous wild type (top) and a heterozygous affected individual (bottom) with the c.2247_2252del; p.(Leu750_Lys751del) *CFH* variant. Arrows represent the beginning and the end of the six deletion nucleotides. **C**: Illustration of reported variants in chromosome 6: chr6:100020205–100143306 duplication, 100,040,906 G>T, 100,040,987 G>C, and 100,041,040 C>T. The red arrow represents the location of the variant identified in the current study within the previously reported hotspot region- a DNase hypersensitivity site (blue), upstream of *PRDM13* gene (green). Genomic localization is based on human reference sequence hg19 (GRCH37). **D**: Chromatograms of a homozygous wild-type (top) and a heterozygous affected individual (bottom) with the chr6: 100040974A>C variant.

| | | | |
|---|---|---|---|
| Human | 714 | SVEFNCSESFTMIGHRSITCIHGVWTQLPQCVAIDKLKKCKSSNLIILEEHLKNKKEFDHNSNIRYRCRGKEGWIHTVCINGRWDPEVNCS-MAQIQL | 810 |
| Chimpanzee | 714 | SVEFNCSESFTMIGHRSITCIHGVWTQLPQCVAIDKLKKCKSSNLIILEEHLKNKKEFDHNSNIRYRCRGKEGWIHTVCINGRWDPEVNCS-MAQIQL | 810 |
| Rhesus monkey | 714 | SVGFNCSESFTMIGHRSITCIHGVWTQLPQCVATDQLKKCKSPNSIVIVENLTSKKEFDHNSTMRYRCRGKGERLHAVCINGRWDPEVTCS-MVQIQL | 810 |
| Dog | 711 | SVEFSCKEEYTMVGPKSITCISGMWTEPPQCIATDELKKC-TYRLTKYEANPLDNIIFDHNDNISYKCRRTLKQKNSTCINGQWDPELTCI-EVEKQS | 806 |
| Cattle | 713 | SVEFSCREAFTMIGPRFITCISGEWTQPPQCIATDELRKCKGSTLFPPEGRQAHKIEYDHNTNKSYQCRGKSEHKHSICINGEWDPKVDCNEEAKIQL | 810 |
| House mouse | 731 | SVEFICEENFTMIGHGSVSCISGKWTQLPKCVATDQLEKCRVLKSTGIEAIKPKLTEFTHNSTMDYKCRDKQEYERSICINGKWDPEPNCT---SKTS | 825 |
| Norway rat | 713 | SVEFTCAETFTMIGHAVVFCISGRWTELPQCVATDQLEKCKAPKSTGIDAIHPNKNEFNHNFSVSYRCRQKQEYEHSICINGRWDPEPNCT-RNEKRF | 809 |

Figure 5. Partial amino acid sequence alignment of the CFH protein. The red box represents the amino acids that were found to be deleted in the present study. Red dots denote the amino acids that are highly conserved among species. Different species (human - NP 000,177.2; chimpanzee - XP 001,136,531.1; Rhesus monkey - XP 001,111,875.1; dog - XP 536,110.2; cattle - NP 001,029,108.1; house mice - NP 034,018.2; and Norway rats - NP 569,093.2) were used to check the conserved amino acids.

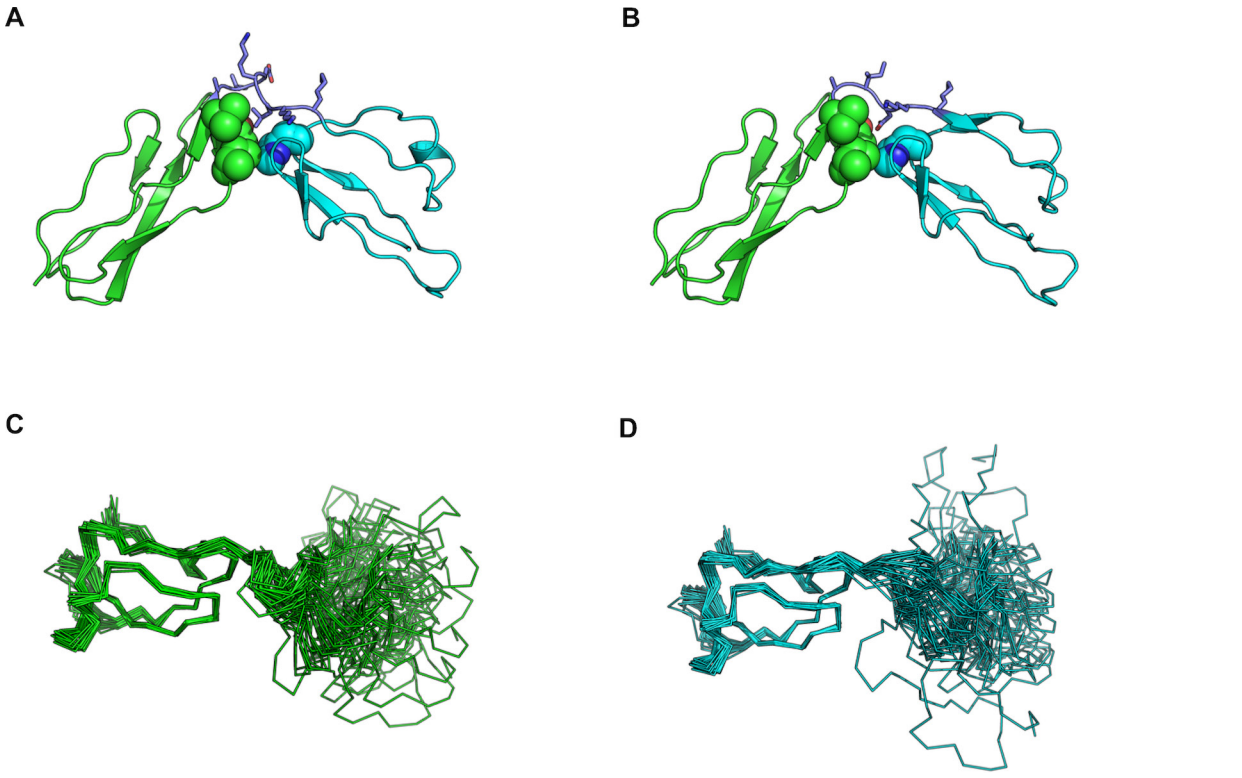


Figure 6. Structure-based analysis of the effect of the L750-K751 deletion. CPP12, linker, and CPP13 colored in green, purple and cyan, respectively. The structure is shown in cartoon, with the linker side chain shown in sticks; residues in the two CPP domains that participate in the formation of the hydrophobic patch are shown in spheres. **A**: Structural model of wt after loop remodeling, highlighting the central position of L750. **B**: Corresponding model of the deletion mutant: in the shortened loop, D748 replaces L750, perturbing the hydrophobic character of this region and leading to destabilization. **C, D**: Different relative orientations adapted by the CPP domains in wt (**C**) and deletion mutant (**D**) indicate increased variability in orientation for the deletion mutant compared to the wt.

of CCPs 12 and 13 [18]. The structure therefore suggests that the defined orientation between the two domains will be disrupted by removing L750. Structural models of the deletion mutant reveal that upon removal of L750-K751, the D748 side chain is positioned at the corresponding L750 site in the wt structure, thereby strongly destabilizing this hydrophobic patch. This could lead to extensive rearrangements (Figure 6B). In silico mutagenesis indicates that the side chain at position 750 mainly contributes to this destabilization. This destabilization can also lead to changes in the relative orientation of the two CCP domains (Figures 6C,D). Therefore, we predict that the identified variation can change the protein structure and may lead to functional consequences that can be a clue regarding the disease occurrence in this family.

The two most common variants in *CFH*, c.1204C > T (rs1061170, p.Tyr402His) [24] and the intronic single nucleotide polymorphism rs1410996 [25], explain 17% of AMD liability. In addition, according to a previous report, p.Arg1210Cys that occurs in CCPs 19–20 and that is predicted to cause loss of function of CFH, similar to our mutation, is likely to drive AMD risk to an earlier onset age of 6 years [26]. This mutation has been associated with extensive macular drusen accumulation and advanced AMD [27]. In addition, AMD patients were found to have a relatively large number of rare variants in CFH in both functional domains, CCPs1–4 and CCPs 19–20 [28].These findings can explain the retinal findings in MOL1154 family members, including confluent drusen, RPE atrophy, and macular atrophy, which constitute typical fundoscopic findings in AMD patients.

The clinical features of the affected individuals of the MOL1154 family are similar to those of previously reported NCMD families [11]. MOL1154 III:1, II:4, and II:2 showed confluent drusen-like clusters within the fovea compatible with grade II NCMD. MOL1154 IV:2 and III:3 presented with macular atrophy compatible with grade III. Following recent reports showing that NCMD can be caused by dysregulation of the retinal transcription factor *PRDM13*, we screened *PRDM13* and its suspected control region for mutations and identified a novel heterozygous transversion (chr6: 100040974A>C). As this variant is located within the previously described suspected control region, we suspect it could be the cause of disease, as supported by the segregation analysis. If we consider 87 YO subject II:1 to have NCMD rather than AMD, then the *PRDM13* segregates in all the affected subjects.

PRDM13 plays a key role in controlling gene expression during development [11,29]. Macular formation is led by differential expression of genes and interaction between transcription factors (such as PRDM13), and the identification of their target genes will contribute to our understanding of this complex process [30]. Any malfunction in this process can lead to macular dysregulation, which causes maculopathy. Variants have also been reported in *CCNC* and *IRX1* in NCMD families, but the role of *IRX1* was not clear with respect to disease pathogenesis [11]. Subsequent studies by Bowne et al. supported the dysregulation of *PRDM13* as the cause of NCMD but not dysregulation of the *CCNC* gene [12]. However, the identification of duplications involving a DNASE1 site near but not involving *IRX1* in the MCDR3 locus in NCMD families suggests that *IRX1* may be a causal target in such cases [9].

In conclusion, NCMD shares important clinical and histopathological features with AMD [13], and therefore finding two different genomic variants in two different unlinked genes may help elucidate the mechanisms underlying these diseases. Because this family represents a rare and likely genetic isolate and because the family is small, it is difficult to be certain of any definitive causality of these findings. The *PRDM13* variant does seem to segregate in all the affected family members if the elderly subject I:2 is considered to be affected with NCMD and not AMD. This variant in the DNASE1 site upstream of *PRDM13* could be a private mutation and a new mutation causing NCMD. Larger families will need to be studied to determine the significance of these variants, particularly the *CFH* variant.

## APPENDIX 1.

To access the data, click or select the words "Appendix 1." A unique *PRDM13*-associated variant in a Georgian Jewish family with probable North Carolina Macular Dystrophy and possible contribution of a unique *CFH* variant.

## ACKNOWLEDGMENTS

The authors thank all affected individuals and family members for their participation in this study. We would like also to thank Nina Schnaider for language editing. The study was financially supported by the United States–Israel Binational Science Foundation (no. 2011202, to D.S. and A.S.). Dr. Eyal Banin (banine@ml.huji.ac.il) and Dror Sharon (dror.sharon1@mail.huji.ac.il) are co-corresponding authors for this study.

## REFERENCES

1. Small KW, Garcia CA, Gallardo G, Udar N, Yelchits S. North Carolina macular dystrophy (MCDR1) in Texas. Retina 1998; 18:448-52. [PMID: 9801042].

2. Lefler WH, Wadsworth JAC, Sidbury JB. Hereditary macular degeneration and amino-aciduria. Am J Ophthalmol 1971; 71:224-30. [PMID: 5100467].

3. Frank HR, Landers MB, Williams RJ, Sidbury JB. A new dominant progressive foveal dystrophy. Am J Ophthalmol 1974; 78:903-16. [PMID: 4440724].

4. Michaelides M, Hunt DM, Moore AT. The genetics of inherited macular dystrophies. J Med Genet 2003; 40:641-50. [PMID: 12960208].

5. Reichel MB, Kelsell RE, Fan J, Gregory CY, Evans K, Moore AT, Hunt DM, Fitzke FW, Bird AC. Phenotype of a British North Carolina macular dystrophy family linked to chromosome 6q. Br J Ophthalmol 1998; 82:1162-8. [PMID: 9924305].

6. Rabb MF, Mullen L, Yelchits S, Udar N, Small KW. A North Carolina macular dystrophy phenotype in a Belizean family maps to the MCDR1 locus. Am J Ophthalmol 1998; 125:502-8. [PMID: 9559736].

7. Small KW, Puech B, Mullen L, Yelchits S. North Carolina macular dystrophy phenotype in France maps to the MCDR1 locus. Mol Vis 1997; 3:1-[PMID: 9238090].

8. Michaelides M, Johnson S, Tekriwal AK, Holder GE, Bellmann C, Kinning E, Woodruff G, Trembath RC, Hunt DM, Moore AT. An early-onset autosomal dominant macular dystrophy (MCDR3) resembling North Carolina macular dystrophy maps to chromosome 5. Invest Ophthalmol Vis Sci 2003; 44:2178-83. [PMID: 12714659].

9. Cipriani V, Silva RS, Arno G, Pontikos N, Kalhoro A, Valeina S, Inashkina I, Audere M, Rutka K, Puech B, Michaelides M, Van Heyningen V, Lace B, Webster AR, Moore AT. Duplication events downstream of IRX1 cause North Carolina macular dystrophy at the MCDR3 locus. Sci Rep 2017; 7:1-9. [PMID: 28790370].

10. Rosenberg T, Roos B, Johnsen T, Bech N, Scheetz TE, Larsen M, Stone EM, Fingert JH. Clinical and genetic characterization of a Danish family with North Carolina macular dystrophy. Mol Vis 2010; 16:2659-68. [PMID: 21179233].

11. Small KW, DeLuca AP, Whitmore SS, Rosenberg T, Silva-Garcia R, Udar N, Puech B, Garcia CA, Rice TA, Fishman GA, Heon E, Folk JC, Streb LM, Haas CM, Wiley LA, Scheetz TE, Fingert JH, Mullins RF, Tucker BA, Stone EM. North Carolina Macular Dystrophy Is Caused by Dysregulation of the Retinal Transcription Factor PRDM13. Ophthalmology 2016; 123:9-18. [PMID: 26507665].

12. Bowne SJ, Sullivan LS, Wheaton DK, Locke KG, Jones KD, Koboldt DC, Fulton RS, Wilson RK, Blanton SH, Birch DG, Daiger SP. North Carolina macular dystrophy (MCDR1) caused by a novel tandem duplication of the PRDM13 gene. Mol Vis 2016; 22:1239-47. [PMID: 27777503].

13. Voo I, Glasgow BJ, Flannery J, Udar N, Small KW. North Carolina macular dystrophy: Clinicopathologic correlation. Am J Ophthalmol 2001; 132:933-5. [PMID: 11730667].

14. Beit-Ya'acov A, Mizrahi-Meissonnier L, Obolensky A, Landau C, Blumenfeld A, Rosenmann A, Banin E, Sharon D. Homozygosity for a novel ABCA4 founder splicing mutation is associated with progressive and severe Stargardt-like disease. Invest Ophthalmol Vis Sci 2007; 48:4308-14. [PMID: 17724221].

15. Das R, Baker D. Macromolecular Modeling with Rosetta. Annu Rev Biochem 2008; 77:363-82. [PMID: 18410248].

16. Stein A, Kortemme T. Improvements to Robotics-Inspired Conformational Sampling in Rosetta. PLoS One 2013; 8:[PMID: 23704889].

17. Kellogg EH, Leaver-Fay A, Baker D. Role of conformational sampling in computing mutation-induced changes in protein structure and stability. Proteins Struct Funct Bioinforma. 2011; 79:830-8. [PMID: 21287615].

18. Schmidt CQ, Herbert AP, Mertens HDT, Guariento M, Soares DC, Uhrin D, Rowe AJ, Svergun DI, Barlow PN. The Central Portion of Factor H (Modules 10–15) Is Compact and Contains a Structurally Deviant CCP Module. J Mol Biol 2010; 395:105-22. [PMID: 19835885].

19. Ripoche J, Day AJ, Harris TJR, Sim RB. The complete amino acid sequence of human complement factor H. Biochem J 1988; 249:593-602. [PMID: 2963625].

20. Sim RB, DiScipio RG. Purification and structural studies on the complement-system control protein β1H (factor H). Biochem J 1982; 205:285-93. [PMID: 6215918].

21. De Córdoba SR, De Jorge EG. Translational Mini-Review Series on Complement Factor H: Genetics and disease associations of human complement factor H. Clin Exp Immunol 2008; 151:1-13. [PMID: 18081690].

22. Estaller C, Weiss EH, Schwaeble W, Dierich M. Human complement factor H: two factor H proteins are derived from alternatively spliced transcripts. Eur J Immunol 1991; 21:799-802. [PMID: 1826264].

23. Schmidt CQ, Herbert AP, Hocking HG, Uhrín D, Barlow PN. Translational Mini-Review Series on Complement Factor H: Structural and functional correlations for factor H. Clin Exp Immunol 2008; 151:14-24. [PMID: 18081691].

24. Haines JL, Hauser MA, Schmidt S, Scott WK, Olson LM, Gallins P, Spencer KL, Kwan SY, Noureddine M, Gilbert JR, Schnetz-Boutaud N, Agarwal A, Postel EA, Pericak-Vance MA. Complement factor H variant increases the risk of age-related macular degeneration. Science 2005; 308:419-21. [PMID: 15761120].

25. Li M, Atmaca-Sonmez P, Othman M, Branham KEH, Khanna R, Wade MS, Li Y, Liang L, Zareparsi S, Swaroop A, Abecasis GR. CFH haplotypes without the Y402H coding variant show strong association with susceptibility to age-related macular degeneration. Nat Genet 2006; 38:1049-54. [PMID: 16936733].

26. Raychaudhuri S, Iartchouk O, Chin K, Tan PL, Tai AK, Ripke S, Gowrisankar S, Vemuri S, Montgomery K, Yu Y, Reynolds R, Zack DJ, Campochiaro B, Campochiaro P, Katsanis N, Daly MJ, Seddon JM. A rare penetrant mutation in CFH confers high risk of age-related macular degeneration. Nat Genet 2011; 43:1232-6. [PMID: 22019782].

27. Ferrara D, Seddon JM. Phenotypic characterization of complement factor H R1210C rare genetic variant in age-related macular degeneration. JAMA Ophthalmol 2015; 133:785-91. [PMID: 25880396].

28. Triebwasser MP, Roberson EDO, Yu Y, Schramm EC, Wagner EK, Raychaudhuri S, Seddon JM, Atkinson JP. Rare variants in the functional domains of complement factor H are associated with age-related macular degeneration. Invest Ophthalmol Vis Sci 2015; 56:6873-8. [PMID: 26501415].

29. Fog CK, Galli GG, Lund AH. PRDM proteins: Important players in differentiation and disease. BioEssays 2012; 34:50-60. [PMID: 22028065].

30. Kozulin P, Natoli R, O'Brien KM, Madigan MC, Provis JM. Differential expression of anti-angiogenic factors and guidance genes in the developing macula. Mol Vis 2009; 15:45-59. [PMID: 19145251].

Articles are provided courtesy of Emory University and the Zhongshan Ophthalmic Center, Sun Yat-sen University, P.R. China. The print version of this article was created on 16 April 2020. This reflects all typographical corrections and errata to the article through that date. Details of any changes may be found in the online version of the article.